



THE UNIVERSITY *of* EDINBURGH

Edinburgh Research Explorer

The Verwey structure of a natural magnetite

Citation for published version:

Perversi, G, Cumby, J, Pachoud, E, Wright, JP & Attfield, JP 2016, 'The Verwey structure of a natural magnetite', *Chemical Communications*, pp. 4864-4867. <https://doi.org/10.1039/C5CC10495E>

Digital Object Identifier (DOI):

[10.1039/C5CC10495E](https://doi.org/10.1039/C5CC10495E)

Link:

[Link to publication record in Edinburgh Research Explorer](#)

Document Version:

Peer reviewed version

Published In:

Chemical Communications

General rights

Copyright for the publications made accessible via the Edinburgh Research Explorer is retained by the author(s) and / or other copyright owners and it is a condition of accessing these publications that users recognise and abide by the legal requirements associated with these rights.

Take down policy

The University of Edinburgh has made every reasonable effort to ensure that Edinburgh Research Explorer content complies with UK legislation. If you believe that the public display of this file breaches copyright please contact openaccess@ed.ac.uk providing details, and we will remove access to the work immediately and investigate your claim.



The Verwey structure of a natural magnetite

G. Perversi,^a J. Cumby^a, E. Pachoud^a, J. P. Wright^b and J. P. Attfield^a

Received 00th January 20xx,
Accepted 00th January 20xx

DOI: 10.1039/x0xx00000x

www.rsc.org/

A remarkably complex electronic order of Fe²⁺/Fe³⁺ charges, Fe²⁺ orbital states, and weakly metal-metal bonded Fe₃ units known as trimers, was recently discovered in stoichiometric magnetite (Fe₃O₄) below the 125 K Verwey transition. Here, the low temperature crystal structure of a natural magnetite from a mineral sample has been determined using the same microcrystal synchrotron X-ray diffraction method. Structure refinement demonstrates that the natural sample has the same complex electronic order as pure synthetic magnetite, with only minor reductions of orbital and trimeron distortions. Chemical analysis shows that the natural sample contains dopants such as Al, Si, Mg and Mn at comparable concentrations to extraterrestrial magnetites, for example, as reported in the Tagish Lake meteorite. Much extraterrestrial magnetite exists at temperatures below the Verwey transition and hence our study demonstrates that the low temperature phase of magnetite represents the most complex long-range electronic order known to occur naturally.

Magnetite, Fe₃O₄, is the original magnetic material and is technologically important in magnetic applications and as the parent phase for spinel ferrites. At ambient temperatures magnetite is ferrimagnetic and has the cubic spinel structure (space group Fd $\bar{3}$ m) with inverse charge distribution Fe³⁺(Fe^{2.5+})₂O₄ over the cation sites of the AB₂O₄ spinel lattice. Early low temperature experiments revealed changes in magnetism, conductivity, and other properties at the Verwey transition, which occurs at T_V ≈ 125 K in pure Fe₃O₄ samples¹. In 1939, Verwey proposed that the transition is driven by charge ordering of Fe²⁺ and Fe³⁺ ions on the octahedral B-sites. However, this order was not verified during the early years of study, and the ground state structure proved controversial for many decades.^{2,3,4,5,6,7,8,9,10,11}

The structure of magnetite below the Verwey transition has an acentric monoclinic $\sqrt{2} \times \sqrt{2} \times 2$ supercell (space group Cc) of the high temperature cubic Fd $\bar{3}$ m spinel arrangement. A full solution of the Cc supercell of highly stoichiometric magnetite was recently achieved through use of microcrystal X-ray diffraction.¹² Fe²⁺/Fe³⁺ charge ordering and orbital ordering of high-spin 3d⁶ Fe²⁺ states (evidenced by Jahn-Teller distortions of the Fe²⁺O₆ octahedra) were found from analysis of the observed Fe-O distances, confirming that the Verwey charge ordering hypothesis is correct to a useful first approximation. However, additional structural distortions in which B site Fe-Fe distances within linear Fe-Fe-Fe units are anomalously shortened showed that electrons are not fully localised as Fe²⁺ states, but are instead spread over the three sites resulting in highly structured three-site polarons known as trimers (Figure 1). These are an example of orbital molecules, weakly-bonded clusters of orbitally-ordered cations^{13,14}.

Charge and orbital orders are known in many transition metal oxides,¹⁵ for example, manganite perovskites such as La_{0.5}Ca_{0.5}MnO₃.¹⁶ However the charge, orbital and trimeron orders of magnetite stand out as perhaps the most complex electron ordered ground state known, and also because magnetite occurs naturally as a common mineral. However, natural magnetites are impure and commonly contain other metals or silicon as dopants that may suppress the electronic order. Previous studies showed that the Verwey transition is very sensitive to non-stoichiometry in Fe_{3(1-δ)}O₄ and Fe_{3-x}M_xO₄ (M = Zn, Ti) cation-doped samples^{17,18,19}. Heat capacity and electrical measurements on single crystals showed that the transition is first order for zero or small impurity levels, and T_V falls from 122 K in pure Fe₃O₄ to 108 K at δ or $x = 0.012$. A broader second order transition is observed above this value where T_V decreases from 101 K to 83 K at the δ or $x \approx 0.035$ upper limit for observation of the Verwey anomaly. Here we investigate whether the long range charge, orbital, and trimeron order previously observed in highly pure Fe_{3(1-δ)}O₄ ($\delta < 0.0001$)¹² is maintained in natural samples with multiply-doped

^a Centre for Science at Extreme Conditions (CSEC) and School of Chemistry, University of Edinburgh, Edinburgh EH9 3FD, UK

^b European Synchrotron Radiation Facility, Grenoble, France

Electronic Supplementary Information (ESI) available: further experimental information and structural results. See DOI: 10.1039/x0xx00000x

compositions comparable to those of extraterrestrial magnetites that exist in the Verwey state.

representative of the bulk in agreement with the chemical analysis.

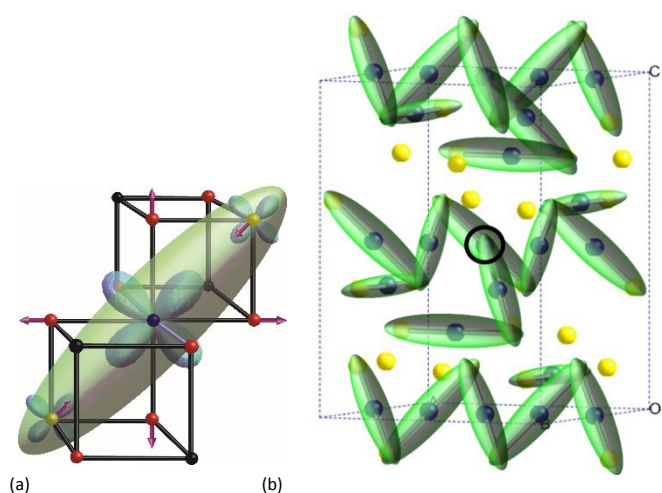


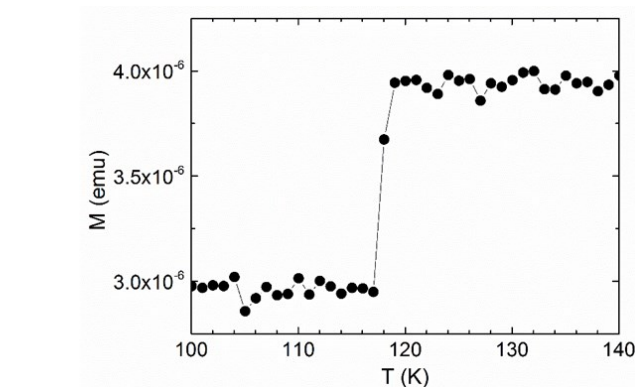
Fig. 1 – (a) A trimeron unit showing the bonding electron density as an ellipsoid with approximate atomic populations indicated by the sizes of the t_{2g} orbitals. The atomic displacement arrows show how orbital order at the central Fe^{2+} site elongates the four Fe-O bonds perpendicular to the local Jahn-Teller axis while weak Fe-Fe bonding shortens the distances to the two adjacent cations. (b) Distribution of charge states (with $\text{Fe}^{2+}/\text{Fe}^{3+}$ states shown as blue/yellow spheres) and trimerons in the low temperature Cc structure of magnetite. Most trimerons are terminated by a Fe^{3+} -type site, but one trimeron ends with Fe^{2+} (circled)

A natural octahedral magnetite crystal of approximate width 1 cm was obtained from the locality of Ouro Preto, Brazil. The crystal was crushed and microcrystal fragments were screened for diffraction quality at room temperature on beamline ID11 at the ESRF synchrotron. A grain of approximate dimensions $60 \times 50 \times 25 \mu\text{m}$ was selected for further study. Electron Probe Microanalysis (EPMA) gave cation contents as shown in Table 1. The sample has a relatively low dopant content (<0.5% total impurities) typical of magnetites of hydrothermal origin, with Al, Si, Mg and Mn as the observed dopants. The microcrystal fragment has a similar composition to the bulk.

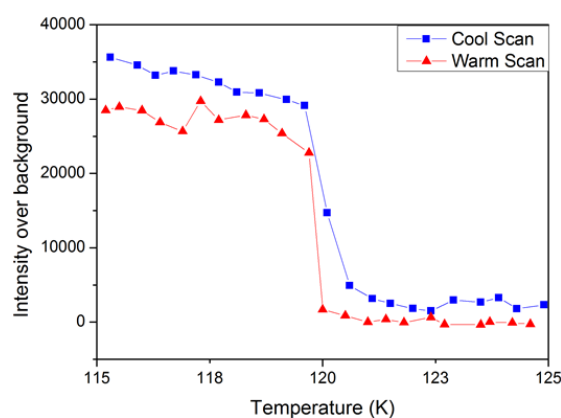
Table 1. Cation compositions from EPMA elemental analysis of the bulk natural magnetite crystal and the microcrystal fragment used for structural study. Compositions are normalised to 3 cations per formula unit and standard deviations in parentheses show compositional variations for the dopants.

Element	Bulk	Microcrystal
Fe	2.9866	2.9888
Al	0.0066(4)	0.0054(4)
Si	0.0030(3)	0.0017(3)
Mg	0.0020(2)	0.0022(2)
Mn	0.0018(6)	0.0019(5)

The Verwey transition of the natural magnetite sample was characterised using SQUID magnetisation and single crystal X-ray diffraction measurements (Figure 2). The microcrystal shows a sharp magnetisation transition at $T_V = 119 \text{ K}$. The bulk powdered sample gives a broader Verwey transition at 116–120 K (shown in ESI), demonstrating that the microcrystal is



(a)



(b)

Fig. 2 – Thermal variations of (a) magnetisation in a field of 500 Oe, and (b) intensity of a superstructure reflection, during cooling and warming scans, for the magnetite microcrystal around the Verwey transition.

A magnetic field was applied to minimise microtwinning of domains while the selected microcrystal was cooled through the Verwey transition, and diffraction images were acquired at 90 K. The presence of a long range structural Verwey transition was revealed by the appearance of sharp superstructure peaks in detector images on cooling, and the temperature evolution of a superstructure intensity shown in Fig. 2(b) confirms the transition at $T_V = 119 \text{ K}$. The natural sample was found to have a monoclinic Cc unit cell with parameters $a = 11.8801(17)$, $b = 11.8457(17)$, $c = 16.7773(30) \text{ \AA}$ and $\beta = 90.267(9)^\circ$ at 90 K. These are similar to those of pure magnetite at the same temperature ($a = 11.88881(3)$, $b = 11.84940(3)$, $c = 16.77515(14) \text{ \AA}$ and $\beta = 90.2363(2)^\circ$)¹² and show that the natural sample has a comparable monoclinic distortion despite impurity doping. The full 90 K data set consists of 45,904 symmetry unique reflections out to a resolution of 0.30 \AA . This enabled coordinates and anisotropic thermal parameters to be refined for all atoms. Domain proportions were also refined and parent domain fraction was found to be 91.9%, with 2.9% of a/-a, 2.8% of a/b, and 2.3% of a/-b twin domains also present. The overall quality of the natural microcrystal is thus very good and comparable to that of pure synthetic magnetite microcrystals studied

previously.^{12,20} The low level of microtwinning of the natural sample may reflect a long annealing period during crystallisation resulting in low residual strains. Further refinement details and results are given as ESI.

Structural evidence for charge ordering of $\text{Fe}^{2+}/\text{Fe}^{3+}$ and orbital ordering of Fe^{2+} states is obtained from the local distortion modes of the B site FeO_6 octahedra in the low temperature structure¹². The amplitude of the radial expansion or breathing mode $Q_{\text{Rad}} = \sum(d_i - d_{\text{av}})/\sqrt{6}$ (summed over the six Fe-O distances d_i in each octahedron, where d_{av} is the global average bond distance) with A_{1g} symmetry is sensitive to charge order, as Fe^{2+} has a larger ionic radius than Fe^{3+} . Q_{Rad} correlates with Bond Valence Sum (BVS) which estimates the formal Fe oxidation state. BVS's were calculated using a standard method²¹ and interpolation formula.⁷ The E_g distortion is doubly degenerate and the amplitudes of the orthorhombic and tetragonal modes were calculated following the procedure used previously.¹² The tetragonal E_g mode with amplitude Q_{JT} describes the compressive Jahn-Teller distortion associated with orbital order of Fe^{2+} , while the non-degenerate $3d^5$ configuration of Fe^{3+} is not Jahn-Teller active.

Figure 3a shows a plot of tetragonal Jahn-Teller Q_{JT} versus breathing Q_{Rad} amplitudes for the 16 crystallographically distinct B sites in the Cc structure of the natural magnetite and the previously-studied highly stoichiometric sample.¹² This enabled the $\text{Fe}^{2+}/\text{Fe}^{3+}$ charge order and Fe^{2+} orbital order to be discovered in the latter material, as the 8 Fe^{2+} -like sites have large Q_{Rad} and significantly negative Q_{JT} values, while the 8 Fe^{3+} -like sites have small Q_{Rad} and near-zero Q_{JT} . The domains of these distributions, shown by the rectangular boxes on Fig. 3a, are very similar for the natural sample, showing that the charge and orbital orders are still present. The Q_{Rad} ranges for the Fe^{2+} and Fe^{3+} like states in the two structures are very similar. However, the Q_{JT} values for the Fe^{2+} and Fe^{3+} like states are more similar to each other in the natural sample than in the stoichiometric material, demonstrating that the orbital order is more sensitive than the charge order to the presence of dopants. Hence this plot shows that while low temperature charge and orbital order in magnetite is sensitive to low levels of doping (<0.5%), long range electronic order is still preserved.

The previous study of a pure magnetite microcrystal at 90 K revealed structural distortions in addition to those from charge and orbital ordering, where distances from Fe^{2+} states to their two B site neighbours (usually Fe^{3+} ions) in the local orbital ordering plane are anomalously shortened due to trimeron formation. 14 of the expected 16 trimeron Fe-Fe contacts are shorter than the average B-B distance. This effect is quantified by the changes $\Delta D_{\text{BB}}(\text{natural})$ of nearest neighbour B-B distances relative to the global average value of 2.9614 Å in the natural sample. To show differences between B-B distances in the natural and pure samples, we plot $\Delta\Delta D_{\text{BB}} = \Delta D_{\text{BB}}(\text{natural}) - \Delta D_{\text{BB}}(\text{pure})$ against $\Delta D_{\text{BB}}(\text{pure})$ in Figure 3b. This plot demonstrates that the trimeron bonding in the natural magnetite sample is very similar to that in the pure sample, with the same pattern of short and long Fe-Fe distances. The magnitude of differences between the two structures ($-0.010 < \Delta\Delta D_{\text{BB}} < 0.015$ Å) is only ~10% of the overall B-B shifts ($-0.20 <$

$\Delta D_{\text{BB}}(\text{pure}) < 0.10$ Å). Relatively large positive values of $\Delta\Delta D_{\text{BB}}$ for trimeron distances show that Fe-Fe bonds which are very short in the pure sample are slightly elongated in the natural material due to the doping effects of impurities. Changes in the non-trimeron B-B distances are smaller and are a consequence of changes in the trimers.

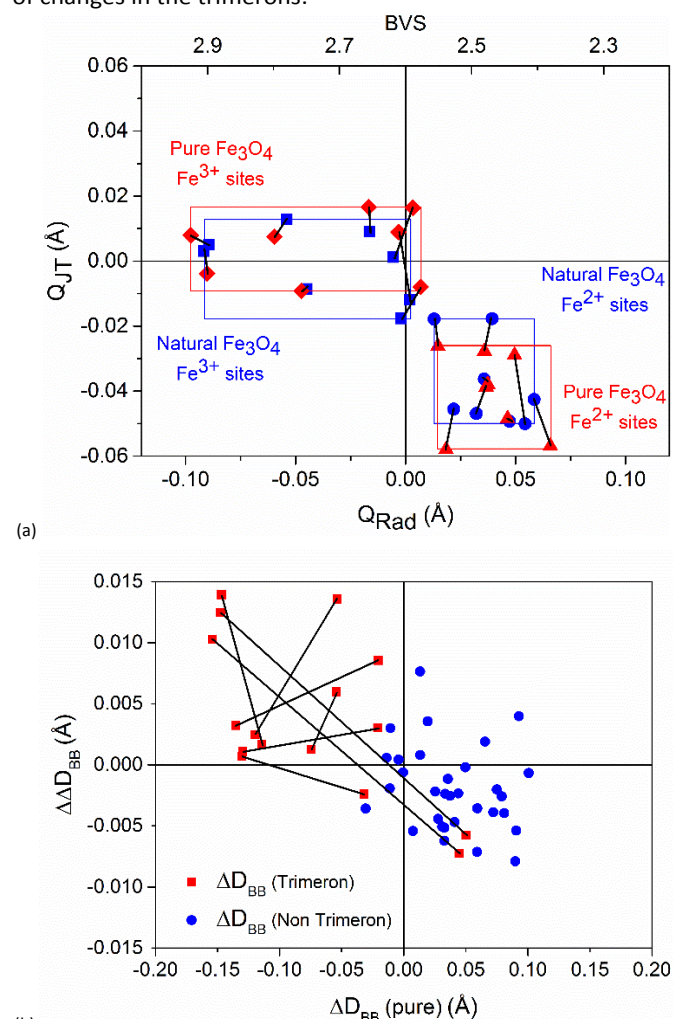


Fig. 3 - (a) Distortion amplitudes of the tetragonal Jahn-Teller (orbital order) mode plotted against the radial (charge order) mode for the 16 octahedral B sites in the Cc structure of the present natural sample and of pure magnetite.¹² Points for the same B-site in the two structures are connected by lines. Domains of the 8 Fe^{2+} -like and 8 Fe^{3+} -like sites are shown as rectangles. An approximate BVS scale is shown at the top of the plot. (b) Plot of $\Delta\Delta D_{\text{BB}} = \Delta D_{\text{BB}}(\text{natural}) - \Delta D_{\text{BB}}(\text{pure})$ against $\Delta D_{\text{BB}}(\text{pure})$, showing changes in the B-B distances relative to those in the pure sample. Different symbols are used for trimeron and non-trimeron distances, and pairs of distances in the same trimeron are connected.

These structural results demonstrate that the complex electronic order of $\text{Fe}^{2+}/\text{Fe}^{3+}$ charges, Fe^{2+} orbital states, and Fe-Fe trimerons discovered in pure synthetic magnetite below the Verwey transition is also present in a microcrystal fragment obtained from a natural crystal typical of aqueous mineralisation. Small differences are observed between the two crystal structures, notably a loss of Fe^{2+} orbital distortions and shortened Fe-Fe trimeron distances in the natural sample due to the dopants. However, the overall long range electronic order is still preserved over a domain scale of a few tens of

microns, as observed in microcrystals of the pure sample. This finding is significant because it demonstrates that the long range electronic order will be present in magnetites of similar chemical compositions at temperatures below the ~ 120 K Verwey transition. Although minerals on Earth are not exposed to temperatures below this limit, much magnetite on other planets, moons, meteors and in grains of space dust is routinely below 120 K. For example, magnetite has recently been identified in a regolith breccia from the Moon, where diurnal temperature variations commonly span T_V .²²

Magnetites that reach Earth in meteorites have varying levels of chemical purity, leading to variations in T_V . Verwey transitions of magnetites from several carbonaceous chondrites (meteorites with high oxide and silicate content, and sometimes also containing water and organic molecules) have been reported from magnetisation measurements.²³ Magnetite from the Tagish Lake meteorite (which has provided a rare example of very primitive solar system materials) was found to have a sharp transition at 122 K which is above that of the natural sample used in this study (with $T_V = 119$ K) and close to that of stoichiometric synthetic material. Hence magnetite within the Tagish Lake meteorite would have been in the electronically-ordered Verwey state prior to falling to Earth. Material from the Orgueil meteorite had a broader transition at $T_V \approx 118$ K but this is also well within the range for long range electronic order. These relatively pure magnetites may have been formed by aqueous alteration within asteroids²⁴ leading to similar dopant levels to terrestrial hydrothermal magnetites such as our Ouro Preto sample. However, magnetites from the Murchison and

Allende meteorites showed no distinct Verwey transition due to relatively high contents of impurities such as Cr that suppress the electronic order.²⁵ Another consequence of the Verwey transition is that the lattice distortion from cubic to monoclinic symmetry gives rise to anisotropic lattice strains²⁶. Hence, the stresses resulting from natural magnetites being cycled through the transition may contribute to mechanical weathering on some planetary bodies.

In summary, the present study shows that long range electronic order is present in slightly doped natural magnetites produced by aqueous processes. Although coupled orders of electronic charges, orbital states and spins are known in many synthetic transition metal compounds, the long-range order within the Verwey state is perhaps the most complex known example and is certainly without comparison amongst naturally occurring substances. The Verwey phase of magnetite thus represents the most complex electronic order known to occur naturally. On a cosmic scale, the Verwey phase is likely to exist widely in cold (<120 K) atomic matter ranging from planets to micron-sized dust particles, given the relatively high abundances of Fe and O.

Notes and references

Open data for this article are at... (link to be added at proof stage).

We thank ERC for funding and STFC for provision of beamtime at ESRF.

¹ E. J. W. Verwey, *Nature*, 1939, **144**, 327.

² M. Iizumi, T. F. Koetzle, G. Shirane, S. Chikazumi, M. Matsui and S. Todo, *Acta Crystallogr. B*, 1982, **38**, 2121.

³ J. P. Wright, J. P. Attfield, and P. G. Radaelli, *Phys. Rev. Lett.* 2001, **87**, 266401.

⁴ J. P. Wright, J. P. Attfield, and P. G. Radaelli, *Phys. Rev. B* 2002, **66**, 214422.

⁵ F. Walz, *J. Phys. Condens. Matter*, 2002, **14**, R285.

⁶ R. J. Goff, J. P. Wright, J. P. Attfield, and P. G. Radaelli, *J. Phys.: Condens. Matter* 2005, **17**, 7633.

⁷ E. Nazarenko, J. E. Lorenzo, Y. Joly, J. L. Hodeau, D. Mannix, and C. Marin, *Phys. Rev. Lett.* 2006, **97**, 056403.

⁸ Y. Joly, J. E. Lorenzo, E. Nazarenko, J. L. Hodeau, D. Mannix, and C. Marin, *Phys. Rev. B* 2008, **78**, 134110.

⁹ J. E. Lorenzo, C. Mazzoli, N. Jaouen, C. Detlefs, D. Mannix, S. Grenier, Y. Joly, and C. Marin, *Phys. Rev. Lett.* 2008, **101**, 226401.

¹⁰ J. Blasco, J. Garcia, and G. Subias, *Phys. Rev. B* 2011, **83**, 104105.

¹¹ J. P. Attfield, *J. Jpn. Soc. Powder Powder Metall.*, 2014, **61**, S43.

¹² M. S. Senn, J. P. Wright and J. P. Attfield, *Nature*, 2012, **481**, 173.

¹³ M. S. Senn, I. Loa, J. P. Wright and J. P. Attfield, *Phys. Rev. B* 2012, **85**, 125119.

¹⁴ J. P. Attfield, *APL Mat.*, 2015, **3**, 041510.

¹⁵ J. P. Attfield, *Solid state sci.*, 2006, **8**, 861.

¹⁶ R. J. Goff and J. P. Attfield, *Phys. Rev. B* 2004, **70**, 140404.

¹⁷ J. M. Honig, *J. Alloys Compd.*, 1995, **229**, 24.

¹⁸ J. P. Shepherd, J. W. Koenitzer, R. Aragón, C. J. Sandberg and J. M. Honig, *Phys. Rev. B*, 1985, **31**, 1107.

¹⁹ J. P. Shepherd, J. W. Koenitzer, R. Aragón, J. Spal and J. M. Honig, *Phys. Rev. B*, 1991, **43**, 8461.

²⁰ M. S. Senn, J. P. Wright, J. Cumby, J. P. Attfield, *Phys. Rev. B*, 2015, **92**, 024104.

²¹ I. D. Brown and D. Altermatt, *Acta Crystallogr. B*, 1985, **41**, 244.

²² K. H. Joy, C. Visscher, M. E. Zolensky, T. Mikouchi, K. Hagiya, K. Ohsumi and D. A. Kring, *Meteorit. Planet. Sci.*, 2015, **50**, 1157.

²³ A. N. Thorpe, F. E. Senftle and J. R. Grant, *Meteorit. Planet. Sci.*, 2002, **37**, 763.

²⁴ J. F. Kerridge, A. L. Mackay and W. V. Boynton, *Science*, 1979, **205**, 395.

²⁵ B. G. Choi, K. D. McKeegan, L. A. Leshin and J. T. Wasson, *Earth Planet. Sci. Lett.*, 1997, **146**, 337.

²⁶ R. S. Coe, R. Egli, S. A. Gilder and J. P. Wright, *Earth Planet. Sci. Lett.*, 2012, **319**, 207.